COMPARISON OF HIRS' EQUATION WITH MOODY'S EQUATION FOR DETERMINING ROTORDYNAMIC COEFFICIENTS OF ANNULAR PRESSURE SEALS†

Clayton C. Nelson and Dung T. Nguyen
Texas A&M University
College Station, Texas 77843

The rotordynamic coefficients of an incompressible-flow annular pressure seal were determined using a bulk-flow model in conjunction with two different friction factor relationships. The first, Hirs' equation, assumes the friction factor is a function of Reynolds number only. The second, Moody's equation, approximates Moody's diagram and assumes the friction factor is a function of both Reynolds number and relative roughness. For each value of relative roughness, Hirs' constants were determined so that both equations gave the same magnitude and slope of the friction factor. For smooth seals, both relationships give the same results. For rough seals ($e/2H_o = 0.05$) Moody's equation predicts 44% greater direct stiffness, 35% greater cross-coupled stiffness, 19% smaller cross-coupled damping, 59% smaller cross-coupled inertia, and nominally the same direct damping and direct inertia.

NOMENCLATURE

C, c	= direct and cross-coupled damping coefficients
D	= diameter
e	= surface roughness height
F_x, F_y	= components of the seal reaction force
f	= Friction factor
H	= seal clearance
K, k	= direct and cross-coupled stiffness coefficients
L	= seal length
M, m	= direct and cross-coupled inertia coefficients
m,n	= Hirs' constants
p	= pressure
Δp	= pressure drop across the seal
$\mathbf{R}$	= Reynold number $(= 2\rho V H/\mu)$
r	= seal radius
t	= time
U_z, U_θ	= fluid velocity in the z and θ direction
V	= fluid velocity
X, Y	= rotor displacement from its geometric center

Z, θ = axial and circumferential seal coordinates
ϵ = eccentricity perturbation
μ = viscosity
ρ = density
ω = shaft angular velocity

Subscripts

$0, 1$ = zeroth and first-order perturbations
x, y = rectangular coordinate directions
s, r = shaft and rotor
z, θ = axial and circumferential coordinate directions

INTRODUCTION

The design and safe operation of today's high-performance turbomachinery require accurate predictions of the hydrodynamic forces developed by annular pressure seals. For small orbital motion of the rotor about its geometric center, the hydrodynamic forces are quantified by specifying a set of linearized rotordynamic coefficients as shown in the following equation.

$$-\begin{Bmatrix} F_x \\ F_y \end{Bmatrix} = \begin{bmatrix} K & k \\ -k & K \end{bmatrix} \begin{Bmatrix} X \\ Y \end{Bmatrix} + \begin{bmatrix} C & c \\ -c & C \end{bmatrix} \begin{Bmatrix} \dot{X} \\ \dot{Y} \end{Bmatrix} + \begin{bmatrix} M & m \\ -m & M \end{bmatrix} \begin{Bmatrix} \ddot{X} \\ \ddot{Y} \end{Bmatrix} \tag{1}$$

In this equation, (X, Y) define the motion of the seal rotor relative to its stator; (F_x, F_y) are the components of the hydrodynamic reactive force acting on the rotor; and (K, k), (C, c), and (M, m) are stiffness, damping and inertia coefficients respectively.

Extensive efforts have been made in the last two decades to theoretically predict, and to experimentally measure these rotordynamic coefficients. Lomakin [1] first demonstrated and explained the characteristic "hydrostatic" stiffness of annular seals for a small displacement from the centered position. Most of the subsequent theoretical developments have been made by Black, Jenssen, Allaire, Fleming, Childs, and Nelson [2-16]. The most recent of these developments by Childs [11-14] (liquid seals) and Nelson [15,16] (gas seals) include the effects of fluid prerotation, convergent-tapered geometry, and different surface roughness treatments for the stator and rotor. Both of these analyses proceed from a single set of governing equations which are based on Hirs' turbulent bulk-flow model [17,18].

Comparison between theoretical and experimental results shows moderately good agreement. However, the theory generally tends to underpredict the experimentally measured direct stiffness. Furthermore, this underprediction appears to get substantially worse as the relative roughness, $e/2H_o$, of the seal increases. This has been found to be true both for liquid seals [13,14,19] and for gas seals [22]. There is, however, a specific need to accurately predict rotordynamic coefficients of seals with very rough stators and/or rotors. To retard leakage, soften the effects of rub, increase damping, and decrease the destabilizing effect of the cross-coupled stiffness, various kinds of intentionally roughened surfaces are being tested and used in liquid and gas seal designs [14,16,23].

Failure of the analysis to predict the correct stiffness may, in part, be due to inadequacies in Hirs' equation for the friction factor. For a given set of Hirs' constants, Hirs' equation can accurately reflect the change in the friction factor for small changes in the Reynolds number, but has no functional dependence on the relative roughness. Nevertheless, the relative roughness does change in the circumferential direction when the rotor is displaced from its centered position.

The results presented in this paper compare the theoretical rotordynamic coefficients obtained by using a bulk-flow analysis in conjunction with two different friction factor relationships. The first relationship is Hirs' equation. The second, Moody's equation, assumes the friction factor is a function of both Reynolds number and relative roughness.

GOVERNING EQUATIONS

Figure 1 illustrates the basic geometry and coordinate system used for the annular pressure seal. Using a bulk-flow model and the control volume shown in Fig. 1, a complete derivation of the governing for compressible flow is given in reference [15]. For incompressible flow, these equations reduce to the following form.

$$\frac{\partial H}{\partial t} + \frac{1}{r}\frac{\partial (HU_\theta)}{\partial \theta} + \frac{\partial (HU_z)}{\partial z} = 0 \tag{2}$$

$$-\frac{H}{\rho}\frac{\partial p}{\partial z} = \frac{U_z}{2}\left(U_z^2 + U_\theta^2\right)^{1/2} f_s + \frac{U_z}{2}\left[U_z^2 + (U_\theta - r\omega)^2\right]^{1/2} f_r + H\left(\frac{\partial U_z}{\partial t} + \frac{U_\theta}{r}\frac{\partial U_z}{\partial \theta} + U_z\frac{\partial U_z}{\partial z}\right) \tag{3}$$

$$-\frac{H}{\rho r}\frac{\partial p}{\partial \theta} = \frac{U_\theta}{2}\left(U_z^2 + U_\theta^2\right)^{1/2} f_s + \frac{(U_\theta - r\omega)}{2}\left[U_z^2 + (U_\theta - r\omega)^2\right]^{1/2} f_r + H\left(\frac{\partial U_\theta}{\partial t} + \frac{U_\theta}{r}\frac{\partial U_\theta}{\partial \theta} + U_z\frac{\partial U_\theta}{\partial z}\right) \tag{4}$$

Hirs' Equation

In the governing equations, f_s and f_r represent the friction factors relative to the stator and the rotor respectively. Hirs' turbulent bulk-flow model assumes that these friction factors can be written as:

$$f = \mathrm{n}\mathbf{R}^{\mathrm{m}} \tag{5}$$

where $\mathbf{R}$ is the Reynolds number relative to the surface upon which the shear stress is acting, and the constants n and m are generally empirically determined from static pressure flow experiments. Substitution of the parameters for the annular pressure seal yields the following equations for the friction factors:

$$f_s = \mathrm{n}_s\left[\frac{2\rho H\left(U_z^2 + U_\theta^2\right)^{1/2}}{\mu}\right]^{\mathrm{m}_s} \tag{6}$$

$$f_r = \mathrm{n}_r\left\{\frac{2\rho H\left[U_z^2 + (U_\theta - r\omega)^2\right]^{1/2}}{\mu}\right\}^{\mathrm{m}_r} \tag{7}$$

Moody's Equation

Figure 2 shows a simplified version of Moody's diagram. Moody produced the following approximate equation for the friction factor [24].

$$f = 0.001375\left[1 + \left(20000\frac{e}{D} + \frac{10^6}{\mathbf{R}}\right)^{1/3}\right] \tag{8}$$

This equation gives values within +5% for Reynolds numbers between 4000 and 10^7 and values of e/D up to 0.01. For $e/D > 0.01$, it significantly underestimates the friction factor. Substituting in the parameters of the annular pressure seal, f_s and f_r become:

$$f_s = 0.001375 \left[1 + \left(10^4 \frac{e}{H} + \frac{5(10)^5 \mu}{\rho H (U_z^2 + U_\theta^2)^{1/2}} \right)^{1/3} \right] \tag{9}$$

$$f_r = 0.001375 \left\{ 1 + \left[10^4 \frac{e}{H} + \frac{5(10)^5 \mu}{\rho H \left[U_z^2 + (U_\theta - r\omega)^2 \right]^{1/2}} \right]^{1/3} \right\} \tag{10}$$

Solution Procedure

Assuming small motion of the rotor about its geometric center, the pressure, density, axial velocity, circumferential velocity, and local seal clearance can be expanded in terms of zeroth-order and first-order perturbation variables.

$$H = H_o + \epsilon H_1, \qquad p = p_o + \epsilon p_1, \qquad U_z = U_{z_o} + \epsilon U_{z1}, \qquad U_\theta = U_{\theta_o} + \epsilon U_{\theta 1} \tag{11}$$

Substitution of these expanded variables into the governing equations (2-4) and either (6, 7) or (9, 10) yields a set of zeroth-order and first-order equations. The nonlinear zeroth-order equations are numerically integrated using a bisection method to obtain matched boundary conditions. The linear first-order equations are expanded from three partial differential equations to twelve ordinary differential equations by assuming that the shaft moves in an elliptical orbit. These twelve ordinary differential equations are then numerically integrated using standard numerical integration techniques. A further integration of the first-order pressures circumferentially and axially over a range of orbital speeds yield the rotordynamic coefficients. Complete details of the solution procedure are given in references [15] and [16].

RESULTS

Seal Parameters

To compare the results of these two friction factor equations, rotordynamic coefficients were determined for a high-pressure water seal defined by the following parameters.

Geometry

length:	$L = 5.08$ cm (2.00 in)
radius:	$r = 7.62$ cm (3.00 in)
nominal clearance:	$H_o = 0.381$ mm (15.0 mil)
nominal relative roughness:	$e/2H_o = 0 \rightarrow 0.05$

Fluid Properties

density:	$\rho = 1000$ kg/m^3 (1.94 slug/ft^3)
viscosity:	$\mu = 1.30(10)^{-3}$ N-s/m^2 $(2.72(10)^{-5}$ lb-s/ft$^2)$

Operating Conditions

Reynolds number:	$\mathbf{R}_o = 30,000$
pressure drop:	$\Delta p = 3.5 \rightarrow 7.0$ MPa (508 $\rightarrow$ 1015 psi)
shaft angular speed:	$\omega = 3000$ rpm
preswirl ratio:	$U_\theta(0,\theta)/(r\omega) = 0.25$

As indicated above, the stator and rotor nominal relative roughness, $e/2H_o$, was varied from 0 to 0.05. To maintain a constant nominal Reynolds number of $\mathbf{R}_o = 30000$, the pressure drop, Δp, was increased along with the roughness. From Moody's diagram, it can be seen that the friction factor varies from $\simeq 0.0056$ to 0.018. This variation is shown by the bold vertical line drawn on the diagram (Figure 2).

For each nominal relative roughness value, a new set of Hirs' constants was determined. These constants were evaluated so that the magnitude and slope of the friction factor from Hirs' equation matched that of Moody's equation. For example, the dashed line on Moody's diagram shows the results of Hirs' friction factor for $e/2H_o = 0.01$.

Rotordynamic Coefficients

The resulting rotordynamic coefficients for the two solutions are shown in Figures 3 - 8. Results from Hirs' equation are shown by the dashed lines, and results from Moody's equation are shown by the solid lines. For smooth seals ($e/2H_o \simeq 0$) both models predict nearly the same values. This result can be explained by observing Moody's diagram. For smooth surfaces, the friction factor curves are close together. That is, changes in relative

roughness for a smooth surface cause only minor changes in the friction factor. Thus, circumferential changes in relative roughness due to rotor displacement are not significant.

As the nominal relative roughness is increased, the most striking difference in the predictions is for the direct stiffness and cross-coupled inertia coefficients. For rough seals, use of Moody's equation results in predicted stiffness coefficients which are 44% greater, and cross-coupled inertia coefficients which are 59% smaller. (Cross-coupled inertia terms are, however, so small that their effect on rotordynamic calculations is rather insignificant.)

The physical explanation for the increase in predicted direct stiffness can easily be seen from Figure 9. As shown, stiffness in annular seals is accounted for by the increase in the axial pressure gradient on the near side of a non-centered rotor. When using Moody's equation, the increased relative roughness on the near side results in a larger friction factor then when using Hirs' equation. This in turn, leads to an even larger pressure gradient.

Finally, use of Moody's equation results in predictions which are 35% greater for cross-coupled stiffness and 19% smaller for cross-coupled damping. Direct damping and direct inertia predictions remain nominally the same.

CONCLUSIONS

As stated in the introduction, there is a specific need to accurately predict rotordynamic coefficients of seals with very rough stators and/or rotors. Annular pressure seals are being tested and used which have surfaces that are honeycombed, grooved, knurled, or contain various sizes and shapes of holes and projections. The ratio of the height of these surface irregularities to the clearance is often close to unity (i.e., $e/2H_o \simeq 1.0$). For these rough seals, the theoretically predicted direct stiffness based on Hirs' equation has been substantially smaller than the measured direct stiffness.

In this analysis, it has been shown that for rough seals, the use of Moody's equation gives significantly larger predictions for direct stiffness than use of Hirs' equation. This occurs even though the magnitude and slope of the nominal friction factors from the two equations are the same. This difference can be explained by the fact that Moody 's equation is a function of both roughness and Reynolds number, while Hirs' equation is a function of Reynolds number only. Thus, Moody's equation can account for the effect of the circumferential changes in relative roughness on the friction factor of a non-centered rotor.

From these results, it would appear that reliable predictions of direct stiffness for rough seals must be based on a more sophisticated model than Hirs' equation. This does not, however, imply that the Moody equation used in this paper is the answer. This equation underestimates the friction factor given in Moody's diagram when $e/2H_o > 0.01$, and the diagram itself gives no values for friction factors when $e/2H_o > 0.05$. Furthermore, the equation does not account for the effect of size, shape, and spacing of large surface irregularities on the friction factor. It is possible, however, that some type of modified Moody's equation could be used. That is, for each type of surface irregularity, friction factor relationships could be determined experimentally and/or analytically. From these relationships, a new set of *Moody constants* could be determined and replace those in Moody's original equation.

REFERENCES

1. Lomakin, A.A., "Calculation of Critical Speed and Securing of Dynamic Stability of Hydraulic High-Pressure Pumps with Reference to the Forces Arising in the Gap Seals," *Energomashinostroenie*, Vol. 4, No. 1, p. 1158.

2. Black, H.F., "Effects of Hydraulic Forces in Annular Pressure Seals on the Vibration of Centrifugal Pump Rotors," *J. Mech. Engr. Sci.*, Vol. 11, No. 2, 1969, pp. 206-213.

3. Jenssen, D.N., "Dynamics of Rotor Systems Embodying High Pressure Ring Seals," *Ph.D. disseration, Heriot-Watt University*, Edinburgh, Scotland, July 1970.

4. Black, H.F., and Jenssen, D.N., "Dynamic Hybrid Properties of Annular Pressure Seals," *Proc. J. Mech. Engr.*, Vol. 184, 1970, pp. 92-100.

5. Black, H.F., and Jenssen, D.N., "Effects of High-Pressure Ring Seals on Pump Rotor Vibrations," ASME Paper No. 71-WA/FF-38, 1971.

6. Black, H.F., Allaire, P.E., and Barrett, L.E., "The Effect of Inlet Flow Swirl on the Dynamic Coefficients of High-Pressure Annular Clearance Seals," Ninth International Conference in Fluid Sealing, BHRA Fluid Engineering, Leeuwenhorst, The Netherlands, Apr. 1981.

7. Allaire, P.E., Gunter, E.J., Lee, C.P., and Barrett, L.E., "The Dynamic Analysis of the Space Shuttle Main Engine-High Pressure Fuel Turbopump. Part II - Load

Capacity and Hybrid Coefficients for the Turbulent Interstage Seals," University of Virginia, Report No. UVA/528140/ME76/103.

8. Fleming, D.P., "High Stiffness Seals for Rotor Critical Speed Control," ASME Paper 77-DET-10, Design Technical Engineering Conference, Chicago Ill., Sept. 26-30, 1977.

9. Fleming, D.P., "Stiffness of Straight and Tapered Annular Gas Seals," ASME Paper 78-LUB-18, ASME-ASLE Joint Lubrication Conference, Minneapolis, Minn., Oct. 24-26, 1978.

10. Fleming, D.P., "Damping in Ring Seals for Compressible Fluids," NASA CP2133, Rotordynamic Instability Problems, in High-Performance Turbomachinery, proceeding of workshop held at Texas A&M University, May 12-14, 1980, pp. 169-188.

11. Childs, D.W., "Dynamic Analysis of Turbulent Annular Seals Based on Hirs' Lubrication Equation," *ASME Trans. J. of Lub. Tech.*, Vol. 105, July 1983, pp. 429-436.

12. Childs, D.W., "Finite-Length Solutions for Rotordynamic Coefficients of Turbulent Annular Seals," *AMSE Trans. J. of Lub. Tech.*, Vol. 105, July 1983, pp. 437-444.

13. Childs, D.W., "Finite-Length Solutions for the Rotordynamic Coefficients of Constant-Clearance and Convergent-Tapered Annular Seals," Third International Conference on Vibrations and Rotating Machinery, York, England, Sept. 10-12, 1984.

14. Childs, D.W., and Kim, C.H., "Analysis and Testing for Rotordynamic Coefficients of Turbulent Annular Seals with Different Directionally Homogeneous Surface Roughness Treatment for Rotor and Stator Elements," accepted for publication, *ASME Trans., J. of Lub. Tech.*

15. Nelson, C. C., "Rotordynamic Coefficients for Compressible Flow in Tapered Annular Seals," *ASME Journal of Tribology*, Vol. 107, No. 3, July 1985, pp 318-325.

16. Nelson, C. C., "Analysis for Leakage and Rotordynamic Coefficients of Surface Roughened Tapered Annular Gas Seals," *ASME Journal of Engineering for Power*, Vol. 106, No. 4, Oct. 1984, pp. 927-934.

17. Hirs, G.G., "Fundamentals of a Fulk-Flow Theory for Turbulent Lubrication Films," *Ph.D. dissertation, Delft Technical University*, The Netherlands, July 1970.

18. Hirs, G.G., "A Bulk-Flow Theory for Turbulence in Lubricant Films," *AMSE J. of Lub. Tech.*, April 1973, pp. 137-146.

19. Childs, D.W., and Dressman, J., "Convergent-Tapered Annular Seals: Analysis and Testing for Rotordynamci Coefficients," accepted for publication in *ASME Trans. J. of Lub. Technology.*

20. Childs, D. W., Nelson, C. C., Nicks, D., Scharrer, J., Elrod, D., Hale, K., "Theory Versus Experiment for the Rotordynamic Coefficients of Annular Gas Seals: Part 1, Test Facility and Apparatus," accepted for publication in *ASME J. of Tribology.*

21. Nelson, C. C., Childs, D. W., "Theory Versus Experiment for the Rotordynamic Coefficients of Annular Gas Seals: Part 2, Constant-Clearance and Convergent- Tapered Geometry," accepted for publication in *ASME J. of Tribology.*

22. Elrod, D., Nicks, C., Childs, D.W, and Nelson, C.C., "A Comparison of Experimental and Theoretical Results for Rotordynamic Coefficients of Four Annular Gas Seals," Progress Report for NASA Lewis Research Center Contract NAS8-33716 prepared by Texas A&M University, #TRC-Seals-5-85.

23. Childs, D. W. and Kim, C. H., "Test Results for Round-Hole Pattern Damper Seals: Optimum Configurations and Dimensions for Maximum Net Damping," ASME Paper No. 85-Trib-16.

24. Massey, B.S., *Mechanics of Fluids*, 4th Ed., Van Nostrand Reinhold Co., New York, 1979.

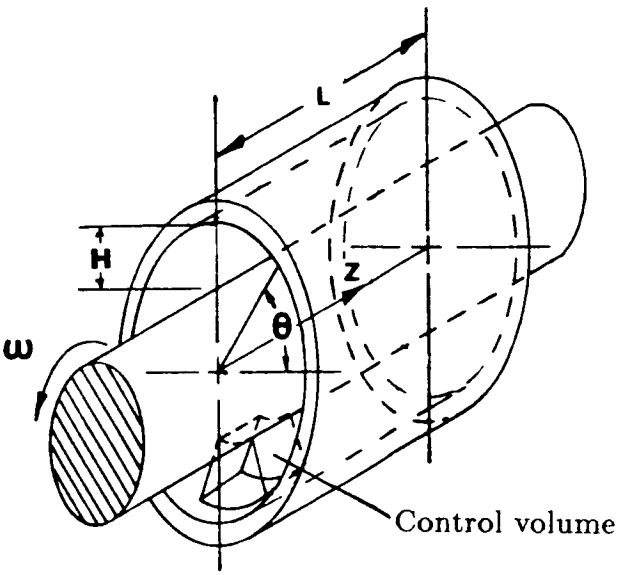

Figure 1. Basic Geometry of the annular pressure seal.

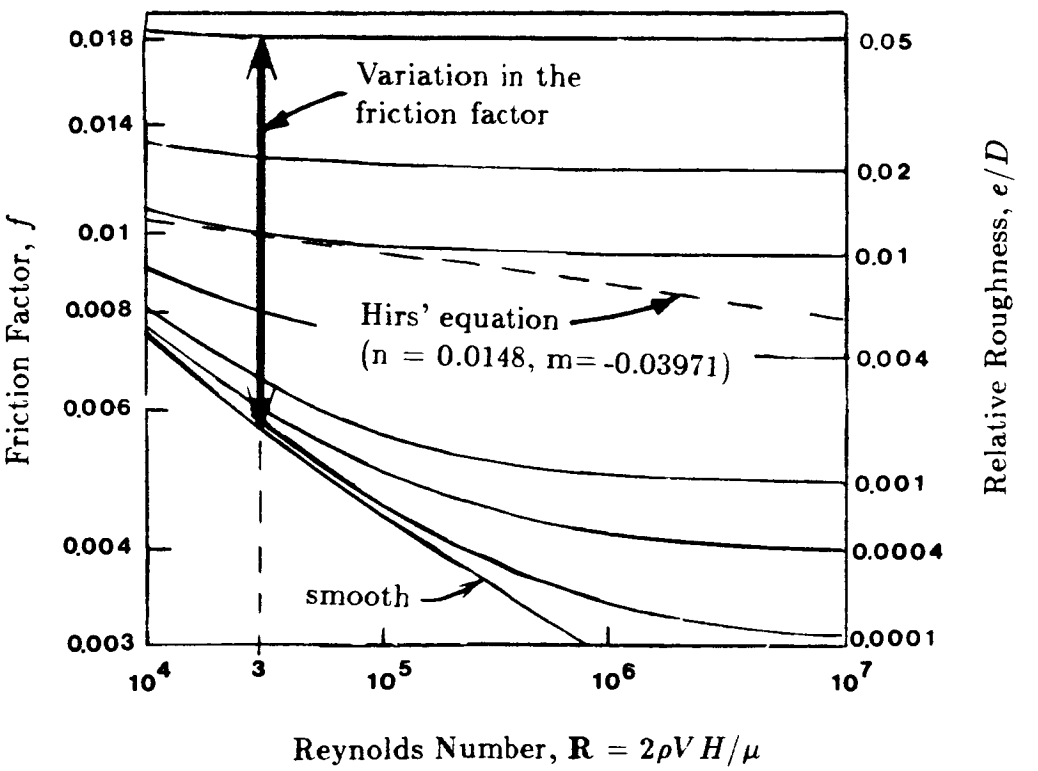

Figure 2. Moody's diagram.

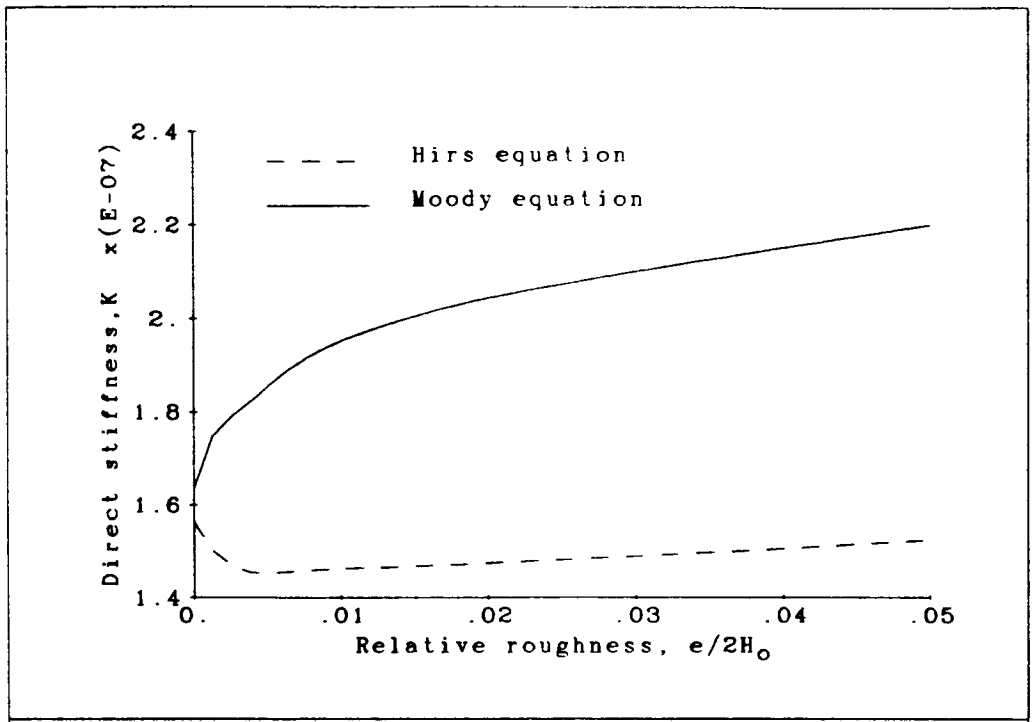

Figure 3. Direct stiffness vs. relative roughness

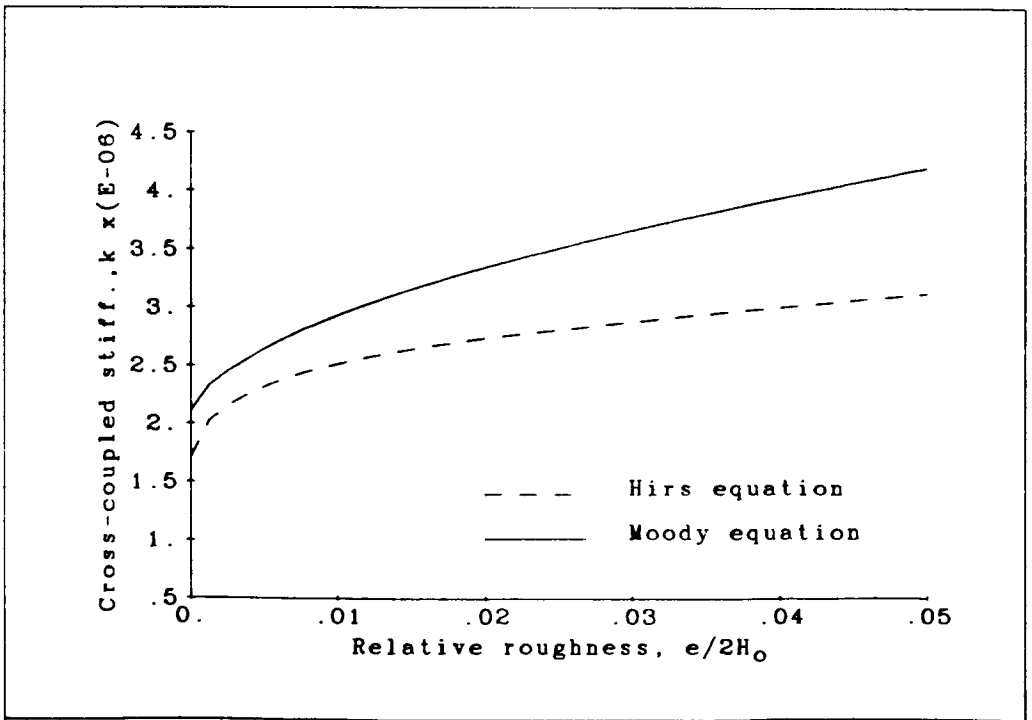

Figure 4. Cross-coupled stiffness vs. relative roughness

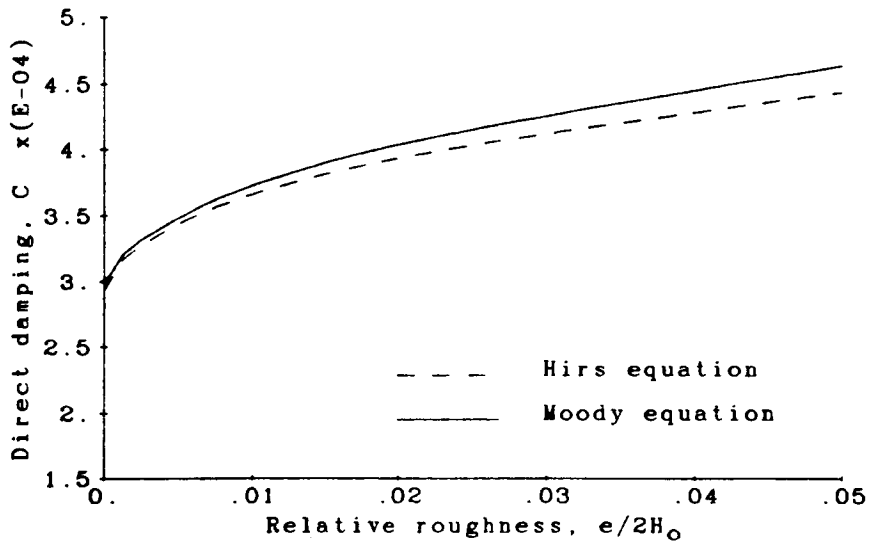

Figure 5. Direct damping vs. relative roughness

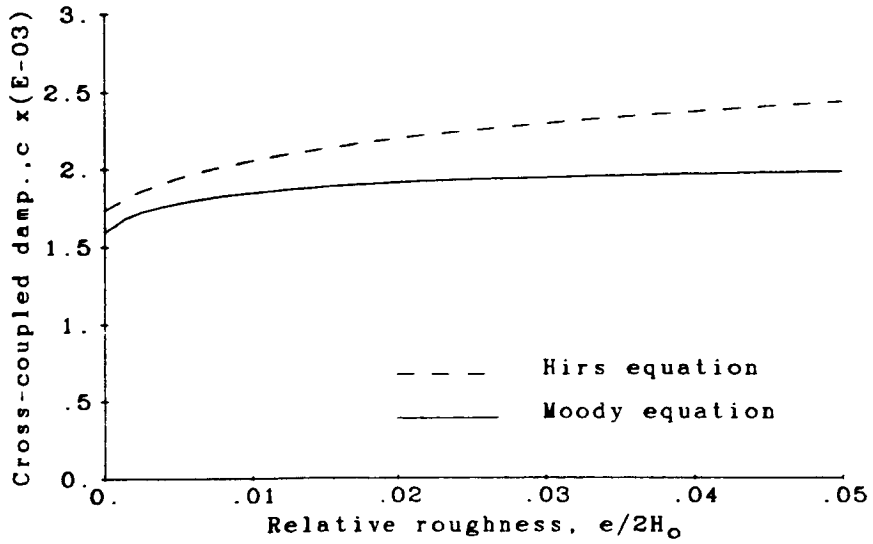

Figure 6. Cross-coupled damping vs. relative roughness

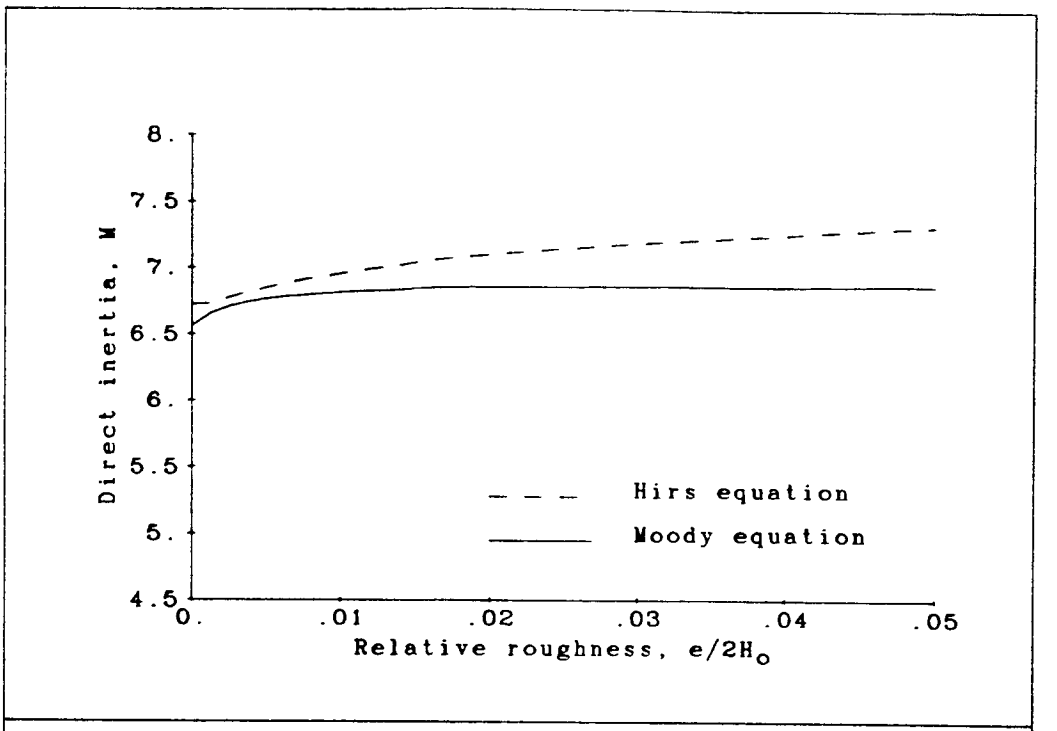

Figure 7. Direct inertia vs. relative roughness

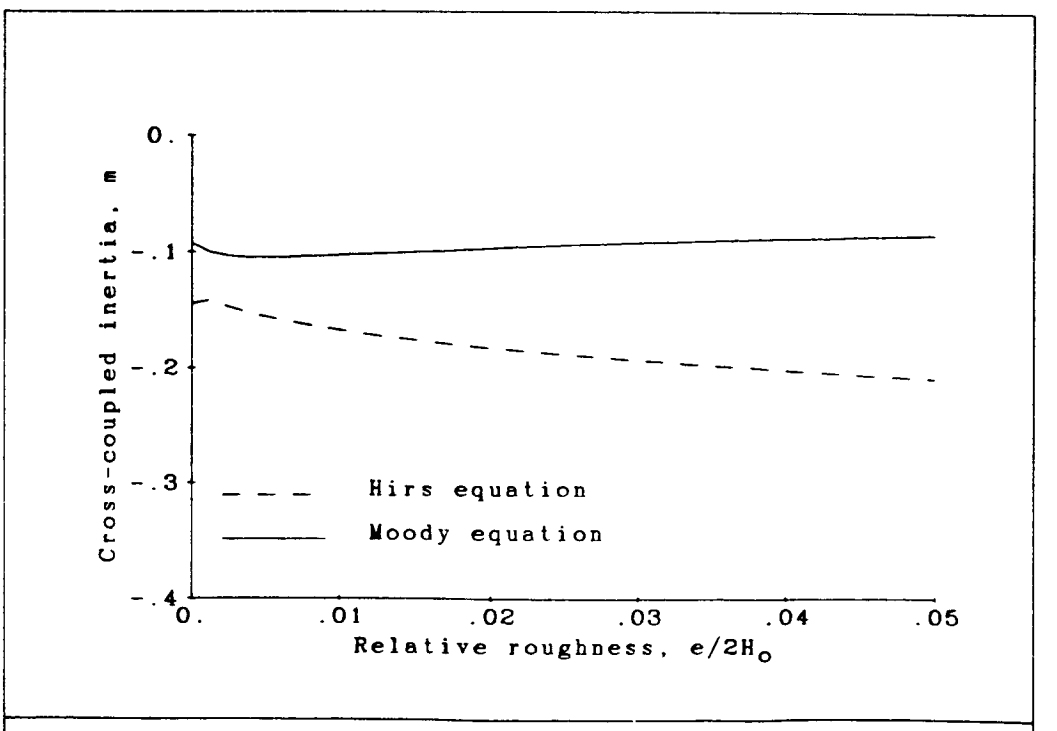

Figure 8. Cross-coupled inertia vs. relative roughness

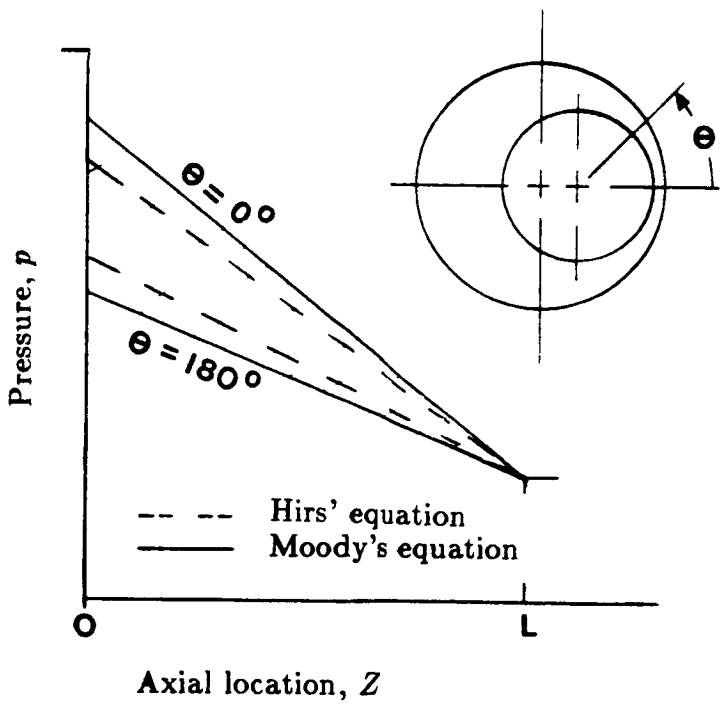

Figure 9. Axial pressure gradient for non-centered rotor.